EVALUATION OF DIFFERENT SUPER-RESOLUTION TECHNIQUES FOR AUTOMOTIVE APPLICATIONS

[1]C. Fischer, [2]F. Ruf, [1]H.-L. Bloecher, [1]J. Dickmann, [2]W. Menzel

[1]Daimler AG, Environment Perception, Wilhelm-Runge-Strasse 11, 89081 Ulm, Germany
[2]University of Ulm, Institute of Microwave Techniques, Albert-Einstein-Allee 41, 89069 Ulm, Germany

Keywords: Automotive Radar, Digital Beamforming, Super-Resolution.

Abstract

This work presents results of the application of different super-resolution techniques to real world scenarios. The sensor used for the measurements utilizes a synthetic aperture with two independent transmit elements. For better exploitation of the given aperture super-resolution techniques are used, namely linear prediction, ESPRIT, MUSIC and Root-MUSIC. These algorithms are compared in simulation with respect to their ability to separate targets and their computational effort. Finally measurement results from scenarios using corner reflectors and real life environment are presented.

1 Introduction

Current development in automotive comfort and safety applications demands for an increasing knowledge about the environment surrounding the car. This knowledge is gained using different kinds of sensors that have very different underlying principles, ranging from ultrasound, over camera to radar systems. As radar sensors have the advantage of being weather independent and can also be installed invisibly behind the bumper, they are the sensor of choice for many of today's functionalities in a car. For installation behind the bumper, space is a crucial point to be considered and sensors have to be built as compact as possible. The antenna aperture is one of the main factors determining the size of a sensor. Functional requirements for angular separation and accuracy demand for larger apertures. Using a synthetic aperture technique with several transmit elements [3] can improve the situation, but progress in modern signal processing hardware, both in speed and in power consumption, enables the potential to exploit a given antenna aperture even more using super-resolution techniques.

This paper presents some of the well-known techniques together with a modern automotive experimental sensor and gives some measurement examples. In the following section the used formalisms are introduced. After that the different algorithms are presented shortly and first simulation results are given. Subsequently the experimental sensor setup and the measurement results are shown. In the end a short conclusion is drawn.

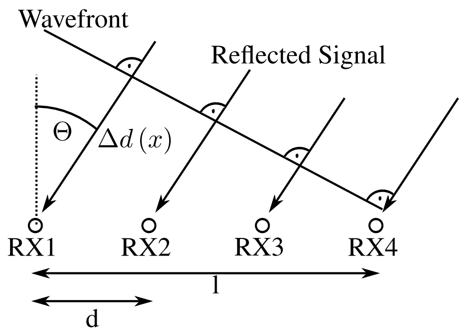

Figure 1: Illustration of a reflected signal impinging on an array of four receivers RX1 to RX4.

2 Data Model

A digital beamforming (DBF) radar uses multiple parallel receive channels with a large field of view (FoV) that are combined using digital signal processing. The input signal can be considered as a spatially sampled version of the incident wave of the reflected transmit signals. Given a certain angle of arrival (AoA) the impinging signal arrives at different times at the receive elements resulting in a phase shift between the receive channels. If the source of the signal is in the far field of the antenna (i.e. the wave is flat) the phase shift increases linearly over the whole aperture (see Figure 1). This results in a harmonic wave sampled at the positions of the receive elements. The frequency of the signal depends directly on the AoA. Therefore it is obvious to use a Fourier Transform (FT) to efficiently determine the incident angle of the signal.

$$f\,(\Theta) = FT\,\{s\,(x)\} \tag{1}$$

This formalism is equivalent to beam steering in a phased array, where the phases of the individual receive channels are adjusted for constructive interference in a certain beam steering angle.

3 Used Techniques

Super-resolution techniques use different mechanisms to decompose frequencies separated less than the resolvable distance determined by the antenna aperture. Subspace methods like MUSIC [6] and ESPRIT [5] use the separation of signal- and noise-spaces defined by the eigenvectors of the covariance matrix of the spatially sampled incident signal. Linear prediction [4] builds a filter model based on the signal to extrapolate it. In the following paragraphs the different methods are presented in more detail.

3.1 Estimation of the Covariance Matrix

For the subspace methods MUSIC and ESPRIT the covariance matrix R of the received signal needs to be estimated. In the noiseless case the matrix R can be calculated directly. In real world the received signal is a superposition of noise and the actual signal and therefore R can only be estimated. The estimation is conducted using

$$R = \frac{1}{N}\mathbf{s}\mathbf{s}^H, \tag{2}$$

with the signal vector $\mathbf{s}$ and the length N of the vector.

3.2 MUSIC and Root-MUSIC

The MUSIC algorithm uses the estimated covariance matrix of a signal to distinguish between the noise space and the signal space. The noise space is defined by a set of eigenvectors of the covariance matrix R that form the matrix E_n. The eigenvectors spanning the signal space form the matrix E_s. Using this separation a pseudo spectrum can be computed by evaluating

$$f\left(\Theta\right) = \left[\mathbf{a}\left(\Theta\right) E_n E_n^H \mathbf{a}\left(\Theta\right)^H\right]^{-1}. \tag{3}$$

This is the approach of the classical MUSIC algorithm. The steering vector $\mathbf{a}\left(\Theta\right)$ has to be evaluated for all possible angles Θ. This search process is also very time-consuming. The term $\mathbf{a}\left(\Theta\right) E_n E_n^H \mathbf{a}\left(\Theta\right)^H$ has zeros at each position of a target, therefore the inverse goes to infinity. This fact results in very sharp peaks in the pseudo spectrum, but on the other hand removes the relation of the peak height to the real amplitude of the target.

When dealing with a uniform, linear array the problem of finding the frequencies of a signal can be transferred to a root finding problem of a polynomial [1]:

$$\mathbf{a}\left(z\right) E_n E_n^H \mathbf{a}\left(z\right)^H = 0 \text{ with } z = \exp\left(\mathrm{j}dk\sin\Theta\right), \tag{4}$$

where d is the distance between the individual antenna elements and k is the wave number. This Root-MUSIC algorithm has the advantage of significantly smaller computational demands besides other advantages shown in section 4 and 6.

3.3 ESPRIT

The ESPRIT algorithm also uses the distinction between signal and noise space. Additionally it demands for two identical but spatially displaced copies of the same antenna configuration. The ESPRIT algorithm exploits the symmetry of these antenna configurations to determine the AoA of an incident signal. The matrices of signal eigenvectors E_1 and E_2 of the two arrays are connected by a matrix Ψ:

$$E_1\Psi = E_2 \tag{5}$$

Therefore the problem of direction finding reduces to the problem to find the matrix Ψ. The eigenvalues of Ψ are then equal to the incident angles of the different signals. In the noiseless case this is a straightforward task. In case of noise, the two matrices do not only differ because of the rotation but also because of different noise influences. The matrix Ψ can then be estimated using different approaches. The least squares (LS) approach assumes that the noise only affects one of the arrays which leads to the estimation

$$\Psi_{LS} = \left(E_1 E_1^H\right)^{-1} E_1^H E_2. \tag{6}$$

There exist other techniques like total least squares (TLS) [5] that assumes both matrices E1 and E2 are affected by noise or structured least squares (SLS) [2] that conserves the structure of the invariance equation (5).

3.4 Linear Prediction

Linear prediction uses an approach different to MUSIC and ESPRIT. The idea behind this algorithm is to take a given signal, build a model and expand the signal's length. After the expansion the signal can be processed like the signal from an array with the expanded size. As a larger array also has a smaller beamwidth, the beamwidth of the virtual array is reduced equally. The advantage of this approach is its linearity. In principle the subsequent signal processing steps are not influenced by the expansion except for the increased length of the signal. Also the relative amplitudes of the individual frequencies contained in it are preserved, what is another vital advantage.

3.5 Estimation of the Number of Targets

For MUSIC and ESPRIT the number of signal eigenvalues and therefore the number of independent frequencies in a signal needs to be known in advance. The most widely used algorithms for this task are the Akaike Information Criterion (AIC) and the Minimum Description Length (MDL) algorithm [8]. Investigations have shown that the MDL algorithm has better performance and has therefore been selected for further consideration. The idea behind it is to find a model that yields minimum code length. The criterion itself is given by

$$MDL = -\log f\left(X|E\right) + 0.5k\log N. \tag{7}$$

The value of $f\left(X|E\right)$ gives the probability for an estimated density E to occur under the observation X, N is the number of observations and k is the number of free parameters in the model.

4 Simulation

For a first estimation of the performance to be expected by the different modes a simple scenario with two targets with equal amplitude positioned at 5° and 10° (Figure 2), and 5° and 11° (Figure 3) has been simulated. The simulated array contains 19 individual elements just like the sensor used for the measurements covered in section 6. Because

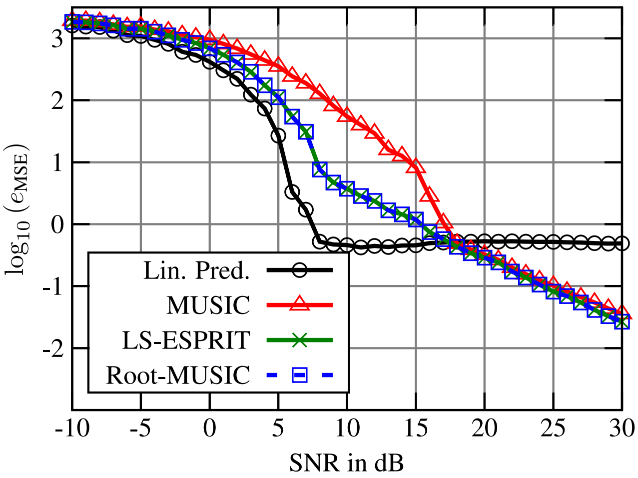

Figure 2: Simulated mean squared error (MSE) of the detected spacing for a scenario with two targets placed at 5° and 10° obtained using 2000 trials for each algorithm and SNR.

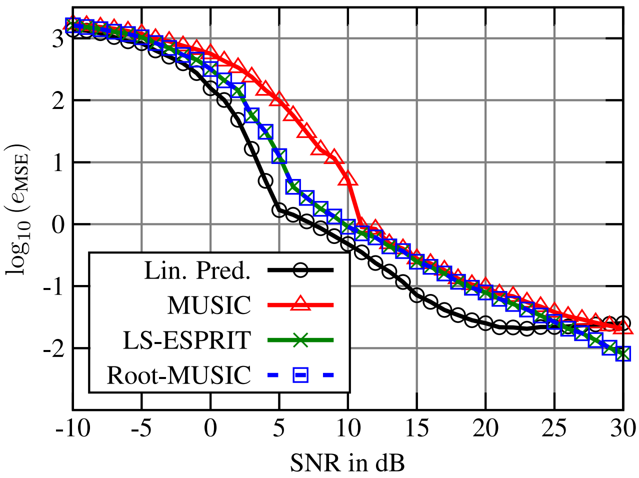

Figure 3: Simulated mean squared error (MSE) of the detected spacing for a scenario with two targets placed at 5° and 11° obtained using 2000 trials for each algorithm and SNR.

of the limited beamwidth the targets could not be resolved using delay and sum beamforming alone. The settings used for the different modes are:

- **Linear Prediction**:
  Two sided with 5 coefficients and expansion by factor 3 to both sides.
- **MUSIC and Root-MUSIC**:
  Covariance Matrix of Dimension 9 with spatial smoothing [7].
- **ESPRIT**:
  Least squares with the two sub arrays ranging from element 1 to 18 and 2 to 19.

The resulting error of the simulation for different SNR values is shown in Figure 2 and Figure 3. To eliminate the influence of outliers the best and the worst percent of the results have been discarded in the evaluation resulting in N=1960 valid data points for averaging:

$$e_{\mathrm{MSE}}\,(\mathrm{SNR}) = \frac{1}{N}\sum_{i=1}^{N}\left(\Delta\hat{\varphi}_i - \Delta\varphi\right)^2 \tag{8}$$

The simulated angle difference is $\Delta\hat{\varphi}$ and the true value is $\Delta\varphi$. The signal to noise ratio (SNR) has been swept in 1 dB steps from -10 to 30 dB. The simulation results in Figure 2 and Figure 3 show the strong dependency on the SNR for the algorithms to give accurate results. For the spacing of 5° in Figure 2 a significantly higher SNR is necessary to give the same error than for the targets with 6° distance in Figure 3. MUSIC needs 5 dB more SNR to give the same accuracy; the other algorithms need 2 to 3 dB. Another striking effect is the observable error floor for the linear prediction in Figure 2: For low SNR the algorithm outperforms the others but above an SNR of about 7 dB remains at the same error level. This cannot be explained by the discretization of the FFT of the expanded signal but is the result of an overlap of the target's spectra shifting the maxima. This effect reduces with increasing separation as can be seen in Figure 3 where the residual error is dominated by the discretization of the frequency grid which is the same for MUSIC and linear prediction. Because of the superior performance of the linear prediction at low SNRs it is ideally suited for environments with few dominant targets and a lot of clutter. For environments with few outstanding reflectors and high Signal-to-Clutter Ratio, ESPRIT or Root-MUSIC appear better suited judging from the present simulation.

The following section introduces the sensor configuration used for the measurements presented in section 6.

5 Used Sensor

The used experimental sensor utilizes a design with two transmitters and 10 parallel receivers. A synthetic aperture can be generated resulting in up to 20 virtual receive channels at 19 different positions. Figure 4 gives an example for a synthetic array with two transmitters and three receivers resulting in five virtual receive channels. The sensor operates in the 76 GHz automotive radar band utilizing 300 MHz of bandwidth resulting in a range resolution of 0.5 m. For range-Doppler-processing the sensor uses a chirp-sequence waveform [9]. Due to the synthetic aperture principle the fast ramps are transmitted alternating between the two antennas therefore reducing the highest measurable Doppler frequency, and equally the maximum measurable velocity, by a factor 2. In the scenario considered here, all targets are static, so only one Doppler cell has been evaluated.

In practice the sensor will be mounted on a car and therefore a relative movement of the sensor to static targets is present in relevant scenarios. As the sensor only measures radial velocities v_r the measured velocity of a target decreases with increasing angle Θ with respect to the moving

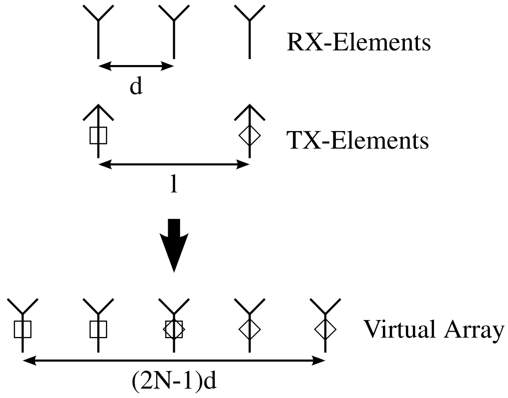

Figure 4: Example for the antenna configuration with a synthetic aperture for three receivers and two transmitters.

direction and the absolute velocity $|\vec{v}|$:

$$v_r = |\vec{v}| \cos \Theta \tag{9}$$

With this, two targets with the same velocity, but different aspect angles have different relative velocities. If this difference in measured, relative velocity is larger than the sensor's Doppler resolution, these targets are already separated in the velocity domain and therefore do not have to be separated in angle. If targets are close to each other the relative Doppler shift may be too small to separate the targets. This means the targets need to be separated by beamforming. As a consequence, sensors with good range and Doppler resolution do not need to separate a high number of targets in angle. The more common use case will be to separate few, but closely spaced targets. This is another important motivation for implementing super-resolution techniques on sensor architectures.

6 Measurement Results

To verify the results of the implemented algorithms two measurement campaigns have been conducted: The first one used two corner reflectors having a defined separation to show the performance of the algorithm in a simple scenario, the other one with a real world scenario to show the algorithms' performance in a not so well defined environment. In the real world scenario the number of signals is estimated using the MDL algorithm as presented in section 3.5. In the scenario with the two corner reflectors the number of signals is set to two. The other parameters have been set as in the simulation in section 4.

6.1 Measurements with Corner Reflectors

For a first comparison of the different super-resolution techniques, a setup with two corner reflectors positioned in the same range cell under different angles has been selected. One corner reflector was positioned at a distance of 10 m directly in front of the sensor (i.e. at 0°) and the other one under different angles below the classical 3-dB-beamwidth. With this setup the ability to separate two point targets under well-known conditions was evaluated. Figure 5 shows one exemplary processing result of the recorded data.

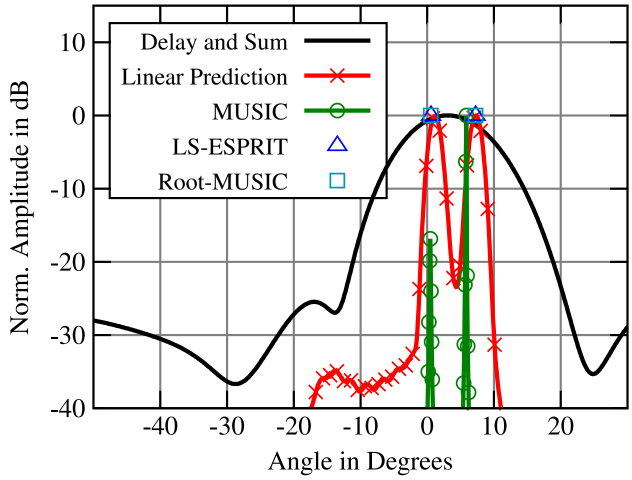

Figure 5: Amplitude plot of five different DOA algorithms. ESPRIT and Root-MUSIC results have been plotted at 0 dB for comparison. The positions of the reflectors are at 0° and 7.5° in 10 m distance to the sensor.

The angle spectra of different processing techniques are displayed. The two reflectors cannot be resolved with the delay and sum approach but with both MUSIC and linear prediction. The MUSIC pseudo spectrum shows the typical spiky character. The amplitudes of the peaks differ by more than 15 dB although the corner reflectors were identical with a radar cross section (RCS) of 10 dBsm. The pseudo spectrum of the linear prediction shows a much smoother shape and also the amplitudes of the two peaks are similar to a very good degree. The fact that the amplitude relation of different targets is not influenced by this type of super-resolution algorithm is an important factor, as the estimated RCS of a target is one vital parameter for object classification. The DOA results for LS-ESPRIT and Root-MUSIC have also been included in the graph to allow better comparison. As these two algorithms in the way implemented here do not give any amplitude information, the resulting angles have been plotted at the 0 dB level (triangle: LS-ESPRIT, square: Root-MUSIC). Summarizing, the estimated angles agree very well.

6.2 Measurements in Real World Scenarios

For further comparison of the presented super-resolution algorithms a real word scenario was evaluated. Figure 6 depicts the scenario. It has been selected because of the diverse reflectors ranging from lamp posts (labeled B and C) with very good, point reflector like behavior, to trees and road signs (labeled A) with a more distributed reflection pattern.
Figure 7 shows the obtained radar image when using the delay and sum algorithm for beamforming. Several strong and isolated reflectors are visible but the broad angular responses prevent a clearer image. The amplitude plot in Figure 8 is based on the same data but uses linear prediction for beamforming. In this radar image several features are visible that have been smeared in the previous plot. Especially the lamp posts B and C appear as point-like targets.

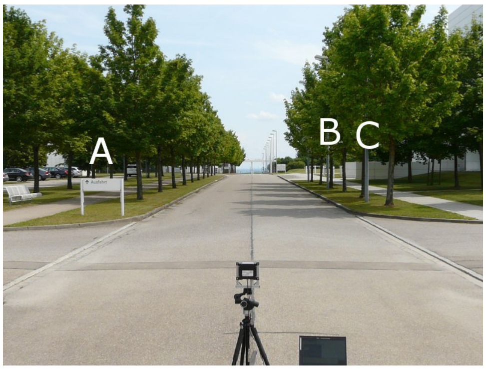

Figure 6: Image of the scene used for the radar image. Strong targets have been marked (A: road sign; B, C: lamp post).

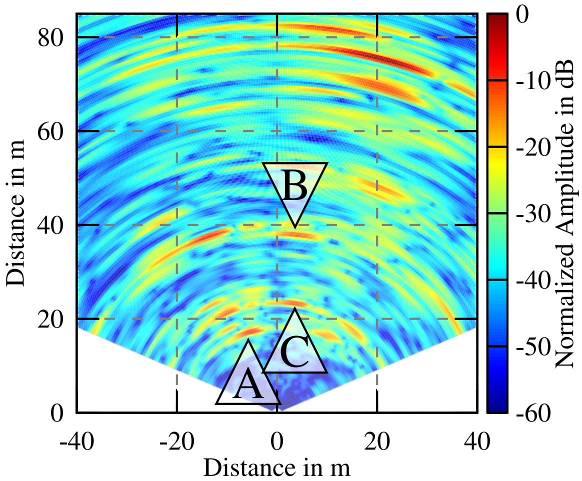

Figure 7: Normalized amplitude plot of a measured scene obtained using the delay and sum algorithm.

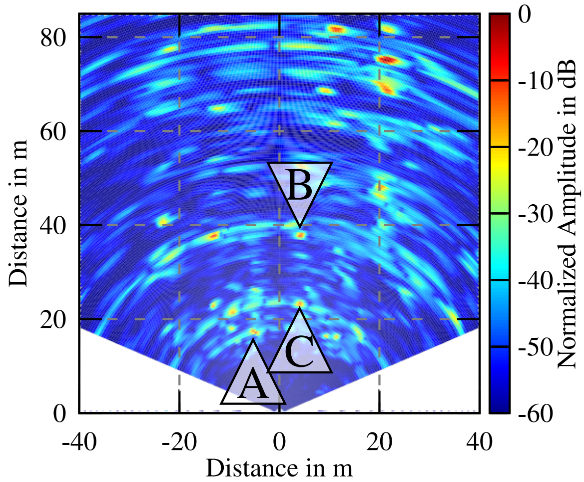

Figure 8: Normalized amplitude plot of a measured scene obtained using the linear prediction algorithm.

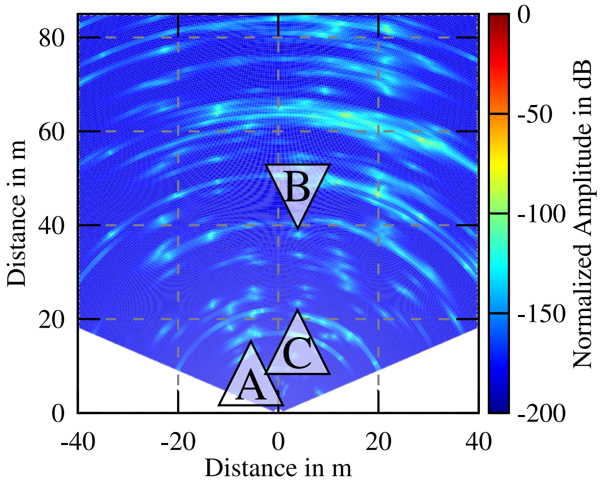

Figure 9: Normalized amplitude plot of the measured scene using the MUSIC algorithm.

Figure 9 displays the beamforming result, when applying MUSIC. The radar image is difficult to interpret as a whole because the relation between the individual targets is lost due to the non-linearity of the pseudo spectrum. Therefore Figure 10 shows the same radar image with a CFAR algorithm applied before the beamforming. In this graph the targets are visible more easily but the nonlinear behavior is still obvious, as the lamp post C has a significantly smaller amplitude as lamp post C. Also some strong false peaks are visible, like the ones right of the marker B. As Root-MUSIC and ESPRIT gave virtually the same results in the simulation only Root-MUSIC is shown in Figure 11. For better mapping to the other graphs Figure 7 has been underlayed. With this combination more details become visible as from the positions alone. This shows that for MUSIC, Root-MUSIC and ESPRIT some knowledge about the environment is necessary in identifying false targets and classifying targets by their reflectivity.

7 Conclusion

In this work several well-known super-resolution algorithms were presented and their performance was evaluated based on a synthetic scenario with two corner reflectors and a real world scenario containing different street objects. Each algorithm was able to improve the result significantly with respect to separability of objects. Concerning computational complexity MUSIC has the highest demand. For imaging radar, especially in an automotive environment with highly dynamic scenarios, its nonlinear behavior complicates the subsequent clustering and object generation task distinctively. The same applies for Root-MUSIC and ESPRIT whereas these have significantly smaller computational complexity. This makes these algorithms an interesting extension for a two stage design: In the first stage a standard beamformer (e.g. delay and sum) computes a low resolution image of the environment, and in the second stage a super-resolution algorithm is applied to the areas, where a higher resolution is desired. Depending on the geometry of the antenna array, this second stage may be ESPRIT or Root-MUSIC.

Linear prediction on the other hand has the advantage of good performance at low SNRs and the linear amplitude

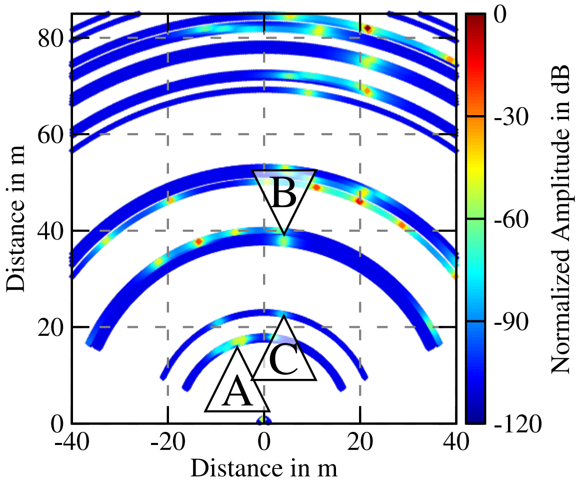

Figure 10: Normalized amplitude plot of the measured scene using the MUSIC and a CFAR algorithm.

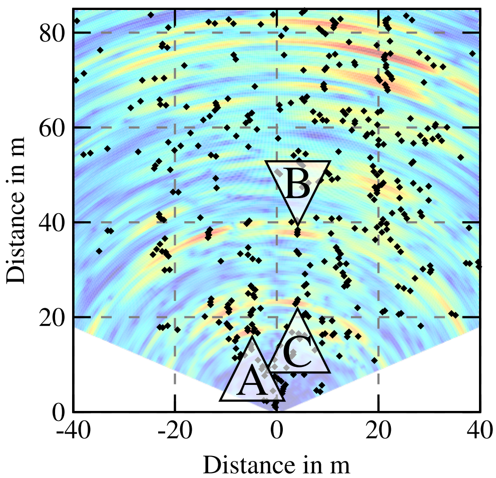

Figure 11: Plot of the measured scene obtained using the Root-MUSIC algorithm. The black dots indicate the target positions obtained by the Root-MUSIC algorithm. Figure 7 has been underlayed for better target mapping.

response enabling the estimation of the environment with high resolution in one processing stage. These properties together with a better runtime than MUSIC, pose an important advantage in highly dynamic environments as they are to be faced in future automotive environments like inner cities.

References

[1] A. Barabell. Improving the resolution performance of eigenstructure-based direction-finding algorithms. In *IEEE International Conference on Acoustics, Speech, and Signal Processing, ICASSP '83.*, volume 8, pages 336–339. IEEE, April 1983.

[2] M. Haardt and J. A. Nossek. Structured least squares to improve the performance of ESPRIT-type high-resolution techniques. In *IEEE International Conference on Acoustics, Speech, and Signal Processing, 1996. ICASSP-96. Conference Proceedings., 1996*, volume 5, pages 2805–2808 vol. 5. IEEE, May 1996.

[3] N. Kees, E. Schmidhammer, and J. Detlefsen. Improvement of angular resolution of a millimeterwave imaging system by transmitter location multiplexing. In *Microwave Systems Conference, 1995. Conference Proceedings., IEEE NTC '95*, pages 105–108. IEEE, May 1995.

[4] J. Makhoul. Linear prediction: A tutorial review. *Proceedings of the IEEE*, 63(4):561–580, April 1975.

[5] R. Roy and T. Kailath. ESPRIT-estimation of signal parameters via rotational invariance techniques. *IEEE Transactions on Acoustics, Speech and Signal Processing*, 37(7):984–995, July 1989.

[6] R. Schmidt. Multiple emitter location and signal parameter estimation. *IEEE Transactions on Antennas and Propagation*, 34(3):276–280, March 1986.

[7] T.-J. Shan, M. Wax, and T. Kailath. On spatial smoothing for direction-of-arrival estimation of coherent signals. *IEEE Transactions on Acoustics, Speech, and Signal Processing*, 33(4):806–811, August 1985.

[8] M. Wax and T. Kailath. Detection of signals by information theoretic criteria. *IEEE Transactions on Acoustics, Speech and Signal Processing*, 33(2):387–392, April 1985.

[9] V. Winkler. Range Doppler detection for automotive FMCW radars. In *Radar Conference, 2007. EuRAD 2007. European*, pages 166–169. IEEE, October 2007.